Available online at www.sciencedirect.com

ScienceDirect

Ceramics International 39 (2013) 9645–9649

CERAMICS INTERNATIONAL

www.elsevier.com/locate/ceramint

Preparation and properties of porous, biomorphic, ceria ceramics for immobilization of Sr isotopes

B. Matovic[a,*], D. Nikolic[a], N. Labus[b], S. Ilic[a], V. Maksimovic[a], J. Lukovic[a], D. Bucevac[a]

[a]*Institute of Nuclear Sciences Vinca, University of Belgrade, PO Box 522, Belgrade, Serbia*
[b]*Institute of Technical Sciences of SASA, Knez-Mihajlova 35/IV, Belgrade, Serbia*

Received 4 March 2013; received in revised form 22 April 2013; accepted 21 May 2013
Available online 28 May 2013

Abstract

A new technology for radionuclide trapping which is based on bio-templating approach was proposed in this paper. Porous oxide ceramics was prepared by wet impregnation of biological template with water solution of cerium and strontium nitrates. The template was derived from linden wood (tilia amurensis). Repeated pressure impregnation, heat treatments and final calcination at 1000 °C in air resulted in the template burnout and consolidation of the oxide layers. The obtained products had structure which corresponded to the negative replication of biological templates. X-ray diffraction, scanning electron microscopy, Raman spectroscopy and porosimetry were employed to characterize the composition and structure of biomorphic ceramics. It was found that the wood impregnated with water solution of cerium and strontium nitrates was converted into oxide ceramics ($Ce_{0.9}Sr_{0.1}O_{2-\delta}$), while preserving the microstructural features of the biological preform.

Keywords: B. Porosity; D. CeO_2; Microstructure; Wood template

1. Introduction

Design of the novel ceramics with specific functional properties and structure by biomimetic approach has recently attained particular attention [1–3]. One of the most important interests is development of materials that are suitable for trapping radioactive waste. The most common processes applied for that purpose involve solidification with inorganic reactants, hydraulic binders such as cement and lime, and immobilization by vitrification and ceramization [4]. Since these types of processes are time and money consuming, the challenge is to design new approaches which allow more convenient methods. One of them is biomimetic approach. The morphology of bioorganic materials is characterized by hierarchically ordered structure ranging from millimeter to nanometer scale. The use of natural biological materials as templates offers the possibility to manufacture novel hierarchical ceramic materials with unique and complex microstructure [5]. So far, several types of biological materials such as diatoms, bacteria, pollen, chitin and wood have been used in order to prepare hierarchical inorganic materials [6–8]. Among them, wood possesses highly anisotropic cellular structure, which can be used as a template to generate novel ceramics with micro-, meso- and macrostructures.

Different kinds of woods were used to manufacture biomorphous SiO_2, TiO_2, Al_2O_3, ZrO_2 ceramics via the sol–gel mineralization or impregnation of pyrolysed wood [9–13]. Among ceramic materials, ceria (CeO_2) is one of the most technologically important materials. It is frequently used as electrolyte for solid oxide fuel cells, catalyst, oxygen sensor and polishing material to name a few [1–4]. Furthermore, ceria is very important as a model material for studying plutonia properties. Ceria and plutonia have quite similar physicochemical properties such as ionic size in octahedral and cubic coordination, melting point, standard enthalpy of formation and specific heat [5–7]. Therefore, the plutonium chemistry could be simulated using ceria instead of highly active PuO_2 [8]. It is worth noting that pure ceria does not undergo phase transformation during cooling from sintering temperature.

*Corresponding author. Tel.: +381 11 3408 753; fax: +381 11 3408 224.
E-mail address: mato@vinca.rs (B. Matovic).

0272-8842/$ - see front matter © 2013 Elsevier Ltd and Techna Group S.r.l. All rights reserved.
http://dx.doi.org/10.1016/j.ceramint.2013.05.086

The high temperature, cubic fluorite structure can be retained on cooling to room temperature which allows fabrication of ceria components without the use of stabilising agents [9]. CeO_2 can also make a stable solid solution with many di- and trivalent ions [10], which makes it suitable for transmutants host material [11,13].

Since the key factor in the preparation of host materials is to tailor and control morphology, the aim of the present paper is to describe the technological approach for the synthesis of biomorphous oxide ceramics for possible application as a host material for radioactive ^{90}Sr isotope storage. According to the authors' knowledge, there is no report on the previous work on the synthesis of biomorphic ceria ceramics with complex chemical composition.

2. Experimental method

Cerium nitrate hexahydrate, $Ce(NO_3)_3 \cdot 6H_2O$, and strontium nitrate, $Sr(NO_3)_2$, produced by Alfa Aesar GmbH, Germany, were used to prepare water solution for wet impregnation. The molar ratio of Ce nitrate and Sr nitrate was 9:1. Linden wood was used as a biological template structure. It is a deciduous wood which exhibits a monomodual pore distribution with a mean pore diameter of about 20 μm. Linden wood was machined into bars ($10 \times 5 \times 5$ mm^3) and dried at 70 °C for 48 h. Dry wood pieces were soaked in 1 M HCl solution to leach lignin out at 60 °C for 48 h and again dried at 60 °C for 48 h. The pressure impregnation was done by placing wood pieces into impregnation vessel and back-filling with the previously prepared water solution of Ce–Sr nitrates. The pressure in the vessel was raised to 5 bars. After being dried at 80 °C for 12 h, the samples were impregnated again with the additional amount of water salt solution. The resultant salt/template composite samples were pyrolysed at 800 °C in nitrogen, for 1 h. Low heating rate (1 °C min^{-1}) was applied for pyrolysis in order to avoid damage of the wood cell walls due to gas release. The main purpose of pyrolysis was to decompose Ce–Sr nitrates and to carbonize wood in order to make space for new amounts of fresh Ce–Sr nitrate solution. This procedure was repeated up to three times to increase the ceramics content in biomorphic samples. The final heat treatment (calcination) was performed in horizontal tube furnace in air at temperature 1000 °C, for 1 h. The intention was to burn carbon and to convert Ce and Sr compounds into oxides. The whole impregnation/heat treatment process is described by the schematic diagram in Fig. 1. Scanning electron microscopy (SEM) analysis was carried out on the untreated sample surface using a JEOL 6300F microscope at 3 kV accelerating voltage. Crystalline phases were identified by X-ray diffraction (XRD) using filtered Cu Kα radiation (Siemens D5000). The Raman spectra were obtained using a U-1000 (Jobin-Ivon) double monochromator in back scattering geometry. The Raman spectra were excited by the 514 nm line of an Ar^+ ion laser and taken at room temperature in the 300–700 cm^{-1} spectral range. The cylindrical focus and laser power were kept lower than 10 mW in order to avoid sample heating. The pore size distribution of the impregnated/heat treated

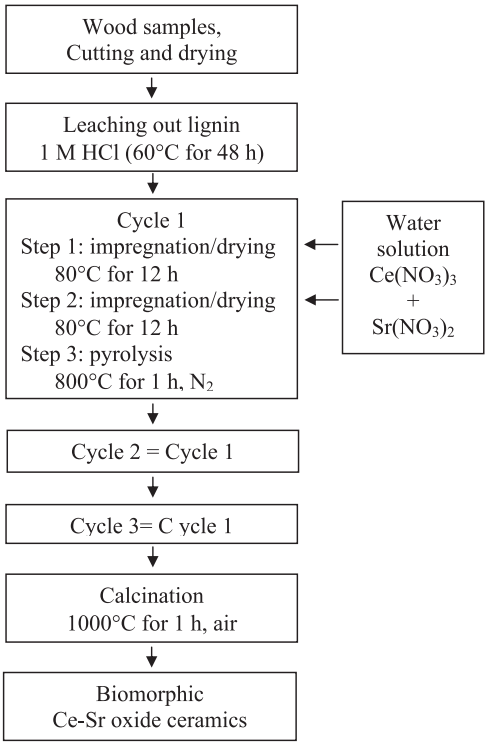

Fig. 1. Flow chart of the manufacturing process for biomorphic Ce–Sr oxide ceramics.

sample calcined at 1000 °C (in air) was determined by means of mercury porosimetry, type PAS-CAL 240/140 (working pressure 1–200 MPa, with minimal pore size detection of 3.7 nm). In addition, BET method was applied to analyze fine pore structure. Geometrical density of obtained ceramic material was determined by measuring weight and volume of the specimens.

3. Results and discussion

The weight gain of the native linden wood during complete (3-cycle) process of impregnation/heat treatment is shown in Fig. 2. One cycle consists of two impregnation/drying steps and subsequent pyrolysis. The weight gain during impregnation/drying steps of each cycle can be explained by the large accumulation of Ce–Sr salts at the inner cell walls of the large vessels. As can be expected the weight gain after the second impregnation/drying step is higher than that after the first impregnation/drying step as the amount of deposited nitrates increases. The lowest weight gain of ~10% was measured in the pyrolysed samples (Cycle 1). Bearing in mind that the weight gain is expressed as a ratio between the weight increase and the weight of starting pieces of wood it can be stated that the weight of samples which are twice impregnated/dried (●) decreases after pyrolysis at 800 °C. The weight loss occurs due to carbonization of wood and decomposition of Ce–Sr salts, probably through evaporation of NO_3 groups. As Fig. 2 evidences, the weight gain constantly increases with the cycle number reaching the value of 16% after the pyrolysis in the third cycle. Knowing that the certain weight loss occurs due to

the carbonization of wood in cycle 1, it can be concluded that the actual weight gain which refers to the increase in amount of infiltrated Ce and Sr is even larger than the measured one.

XRD pattern of the impregnated/heat treated sample calcined at 1000 °C (in air) is shown in Fig. 3. The role of calcinations was to remove residual carbon and to convert Ce and Sr compounds into oxides. The pattern shows only reflections of ceria, which can be indexed on the fluorite space group (S.G. 225). Since the peaks related to isolated Sr-phases are not observed, it can be assumed that Sr is incorporated in CeO_2 phase. Dissolution of the Sr ion in the lattice causes shifting of the peaks toward the lower angles indicating the existence of a solid solution. According to Shannon's compilation, the ionic radii of Ce^{4+} and Sr^{2+} for coordination number 8 are 0.97 and 1.26 Å, respectively. Thus, doping with larger sized Sr^{2+} ions will enlarge the cell lattice. The measured value of lattice parameter of doped sample calculated according to the ion-packing model is 5.4149 Å, and corresponds to the $Ce_{0.9}Sr_{0.1}O_{2-\delta}$ phase [14,15] which is in a good agreement with the composition of starting Ce–Sr nitrates solution.

As mentioned before, $Ce_{1-x}Sr_xO_{2-\delta}$ phase has a fluorite structure and only a single Raman mode is allowed with F_{2g} symmetry [16]. The feature is observed as a symmetric breathing mode of the O atoms around each Ce^{4+} cation. In ceria this frequency is around 465 cm^{-1}. However, in the Raman spectra, presented in Fig. 4, the new mode peak appears at 545 cm^{-1}. This mode is attributed to the presence of additional O^{2-} vacancies that were introduced into the ceria lattice by substitution of Ce^{4+} ions with Sr^{2+} ions in order to keep the charge neutrality. Additional mode also appears at about 600 cm^{-1} which is assigned to intrinsic oxygen vacancies [17].

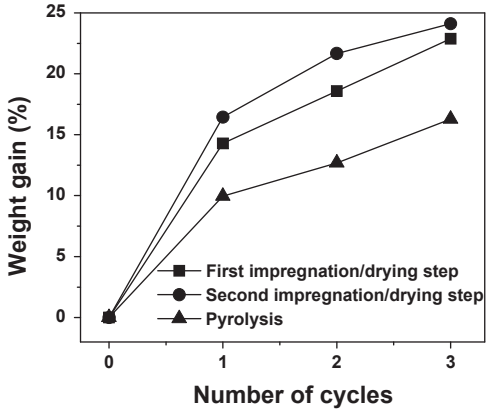

Fig. 2. Weight gain as a function of number of cycles. ■ is the weight gain after the first impregnation/drying step of each cycle, ● is the weight gain after the second impregnation/drying step and ▲ is the weight gain after pyrolysis at 800 °C. The weight gain was calculated as a ratio between the weight increase and the weight of starting pieces of wood.

The morphology of impregnated linden wood after calcination at 1000 °C is shown in Fig. 5. The microstructure features of wood samples such as tracheidal pore channels and pits are well visible in Fig. 5b–d. It is believed that the pore channels come from the cellulose fibers which were originally imbedded in lignin. After the lignin was leached out by HCl the wood microstructure was mainly consisted of cellulose fibers. The pore channels were obtained by burning the carbon residue of cellulose during calcination in air. It is important to note that Fig. 5a does not show any signs of desintegration of calcined samples. As Fig. 5b indicates the diameter of the obtained pore channels ranging from 20 to 100 μm which implies that the microstructure of wood was preserved during impregnation/drying/pyrolysis steps. Furthermore, Fig. 5c, which shows microstructure under high magnification, reveals the presence of narrow pore channels with diameter bellow 10 μm. Finally, Fig. 5d reveals the presence of even smaller pore channels with diameter of few microns which are located in the cellular wall. It is also evident that the reaction between carbon template and oxides did not take place in the cellular wall at 1000 °C. Conversion of Ce and Sr salts into oxides and their consolidation was done while the microstructural features of the biological preform were preserved.

Having concluded that channel diameter varies from few microns to 100 μm it would be of great importance to analyze the pore size distribution. The pore size distribution of the impregnated/heat treated sample calcined at 1000 °C (in air) was determinated by Hg porosimetry and presented in Fig. 6. As the figure shows, the curve ehxibits two peaks. The first one is around 50 μm whereas the second one is located between 70 and 80 μm. This is in a good agreement with

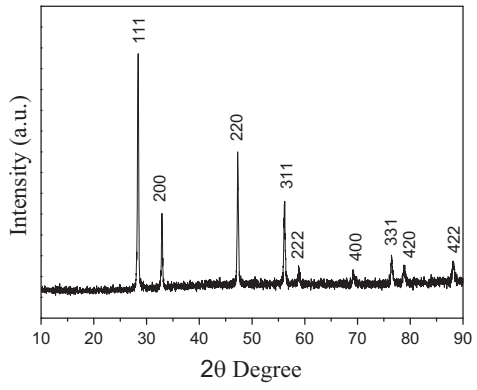

Fig. 3. XRD pattern of impregnated/heat treated sample after 1-h long calcination at 1000 °C in air.

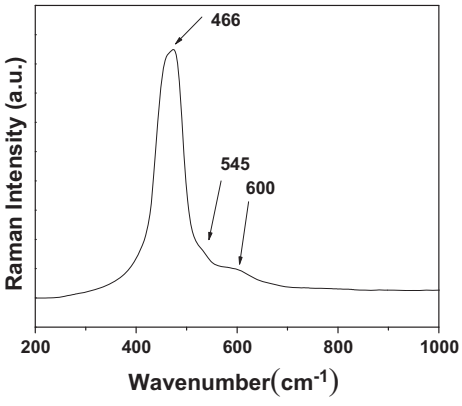

Fig. 4. Raman spectra of impregnated/heat treated sample after 1-h long calcination at 1000 °C in air.

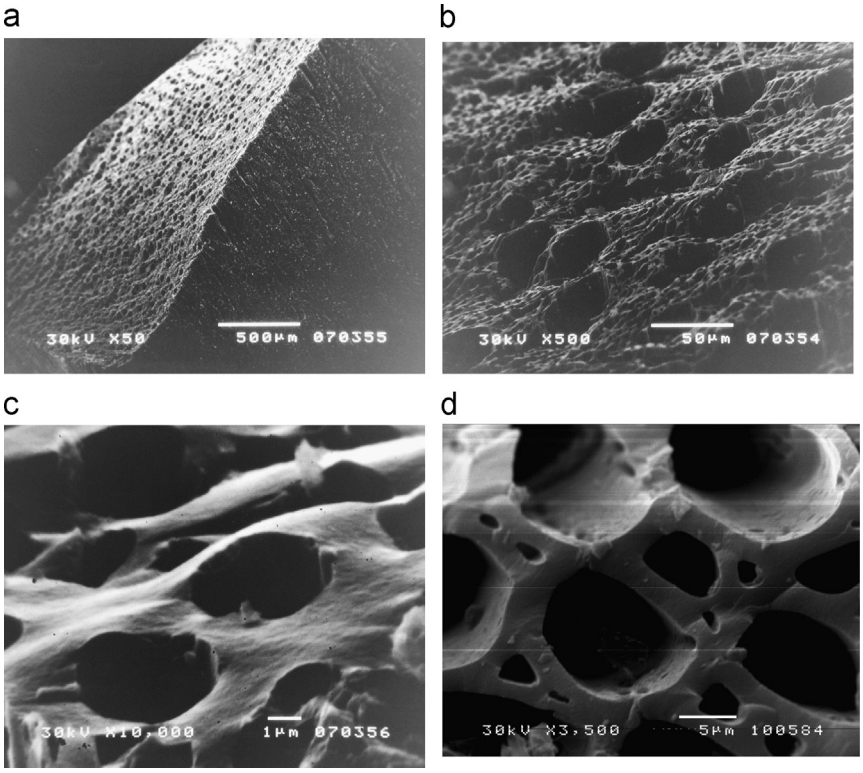

Fig. 5. SEM micrographs of impregnated/heat treated sample after 1-h calcination at 1000 °C in air; (a) 3D image, (b) and (c) surface images, (d) bimodal pore size distribution.

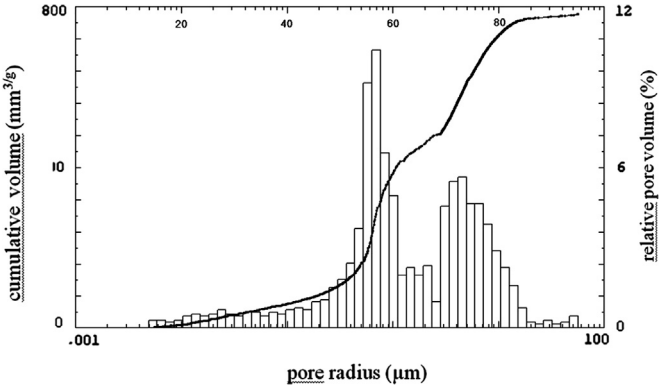

Fig. 6. Hg porosimetry—Pore size distribution of impregnated/heat treated sample after 1-h long calcination at 1000 °C in air.

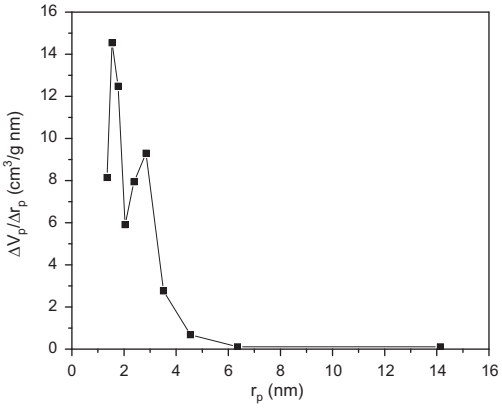

Fig. 7. BET porosimetry—Fine pore structure of impregnated/heat treated sample after 1-h long calcination at 1000 °C in air.

SEM investigation which showed that the majority of pore channels have diameter of ~50 µm (Fig. 5b) with certain number of channels with somewhat larger diameter. Although the sample shows macroporous nature, the results of BET analysis reveal the significant presence of nanosized pores. Fig. 7 shows that pore size radius varies between 2 and 6 nm, with two sharp peaks around 2 and 3 nm. According to IUPAC classification these pores are considered as mesopores (2–50 nm) [18]. It is believed that the mesopores are located in the walls of porous structure giving them considerable mesoporosity. The overall porosity was found to be ~44% which is in a good agreement with SEM observation. The density of calcined material was 4.03 g/cm^3 which corresponds to 56% of the theoretical density of composition $Ce_{0.9}Sr_{0.1}O_{2-\delta}$.

4. Conclusions

The successful conversion of the biological tissue with cellular structure into porous ceramics was demonstrated. The porous Ce-oxide ceramics with wood-like microstructure were prepared by process consisting of impregnation of linden wood with water solution of Ce and Sr nitrates, drying, pyrolysis and subsequent calcinations at 1000 °C. Macroporous biomorphic ceramics with certain amount of mesoporosity

was obtained. XRD and Raman spectroscopy revealed that the obtained Ce-oxide ceramics was monophase solid solution with $Ce_{0.9}Sr_{0.1}O_{2-\delta}$ composition. It appears that ceria can be used as a host material for storage of radioactive ^{90}Sr isotope.

Acknowledgment

This project was financially supported by the Serbian Ministry for Education and Science (projects number: TR37021).

References

[1] S. Mann, Biomimetic Materials Chemistry, VCH Publishers, New York, 1996.
[2] P. Greil, T. Lifka, A. Kaindl, Journal of the European Ceramic Society 18 (1998) 1961–1973.
[3] O.P. Chakrabarti, H.S. Maiti, R. Majumdar, Bulletin of Materials Science 27 (2004) 467–470.
[4] P. Cappelletti, G. Rapisardo, B. Gennaro, A. Collela, A. Langella, S.F. Graziano, D.L. Bish, M. Gennaro, Journal of Nuclear Materials 414 (2011) 451–457.
[5] S.A. Davis, M. Breulmann, K.H. Rhodes, B. Zhang, S. Mann, Chemistry of Materials 13 (2001) 3218–3236.
[6] P. Greil, Journal of the European Ceramic Society 21 (2001) 105–118.
[7] H. Sieber, Materials Science and Engineering A 412 (2005) 43–47.
[8] B. Matovic, A. Saponjic, S. Boskovic, Journal of the Serbian Chemical Society 71 (6) (2006) 677–683.
[9] S. Yongsoon, S. Yun, H.C. Jeong, N. Zimin, G.J. Exarhos, Advanced Materials 13 (2001) 728–732.
[10] T. Ota, M. Imaeda, H. Takase, M. Kobayashi, N. Kinoshita, T. Hirashita, H. Miyazaki, Y. Hikichi, Journal of the American Ceramic Society 83 (2000) 1521–1523.
[11] J. Cao, O. Rusina, H. Sieber, Ceramics International 30 (2004) 1971–1974.
[12] J. Cao, C.R. Rambo, H. Sieber, Journal of Porous Materials 11 (2004) 163–172.
[13] M. Singh, B.M. Yee, Journal of the European Ceramic Society 24 (2004) 209–217.
[14] S.J. Hong, A.V. Virkar, Journal of the American Ceramic Society 78 (1995) 433.
[15] B. Matovic, S. Boskovic, L.J. Zivkovic, M. Vlajic, M.V. Krstić, Materials Science Forum 494 (2005) 175–180.
[16] J.R. McBride, K.C. Hass, B.D. Poindexter, W.H. Weber, Journal of Applied Physics 76 (1994) 2435–2441.
[17] J.R. McBride, K.C. Hass, B.D. Poindexter, W.H. Weber, Journal of Applied Physics 76 (1994) 2435.
[18] S. Lowell, J.E. Shields, M.A. Thomas, M. Thommes, Characterization of Porous Solids and Powders: Surface Area, Pore Size and Density, Kluwer Academic Publisher, Dordrecht Netherland, 2004, pp. 44–57.